

2,3,7,8-Tetrachlorodibenzo-*p*-dioxin Activation of the Aryl Hydrocarbon Receptor/Aryl Hydrocarbon Receptor Nuclear Translocator Pathway Causes Developmental Toxicity through a CYP1A-Independent Mechanism in Zebrafish

Sara A. Carney, Richard E. Peterson, and Warren Heideman

Molecular and Environmental Toxicology Center (S.A.C., R.E.P., W.H.) and School of Pharmacy (R.E.P., W.H.), University of Wisconsin, Madison, Wisconsin

Received February 23, 2004; accepted May 21, 2004

This article is available online at <http://molpharm.aspetjournals.org>

ABSTRACT

The aryl hydrocarbon receptor (AHR) is a ligand-activated transcription factor that dimerizes with ARNT to mediate responses to compounds such as 2,3,7,8-tetrachlorodibenzo-*p*-dioxin (TCDD). TCDD and other AHR agonists cause toxic responses in early life stages of fish, including the zebrafish, *Danio rerio*. The most well characterized target gene for the AHR/aryl hydrocarbon receptor nuclear translocator (ARNT) dimer is a cytochrome P450, CYP1A. Induction of CYP1A by TCDD has been correlated with certain toxic responses in developing zebrafish and has been postulated to mediate these responses. To determine whether CYP1A is the important downstream effector enzyme for the AHR/ARNT pathway, we used morpho-

lino oligonucleotides (MOs) to block induction of CYP1A in response to TCDD in zebrafish embryos. Although the *zfcyp1a*-MO effectively prevented CYP1A up-regulation, it did not prevent the signs of developmental toxicity, including pericardial edema, slowed blood flow, craniofacial malformation, and defects in erythropoiesis. We conclude that the important target for the AHR/ARNT pathway in developing zebrafish exposed to TCDD is not *zfcyp1a*. This suggests an alternative model in which TCDD-activated AHR/ARNT disrupts the normal process of growth and development by altering programs of gene expression or function.

Embryonic exposure to 2,3,7,8-tetrachlorodibenzo-*p*-dioxin (TCDD), a widespread environmental contaminant, causes systemic toxicity during embryonic development in many fish species. Exposure to TCDD causes cardiovascular dysfunction, edema, hemorrhage, craniofacial malformation, anemia, and mortality in developing fish (Walker and Peterson, 1994; Henry et al., 1997; Belair et al., 2001; Tanguay et al., 2003).

TCDD causes toxicity through activation of the aryl hydrocarbon receptor (AHR) pathway (Schmidt and Bradfield, 1996). TCDD binding to AHR causes its translocation to the nucleus and dimerization with the aryl hydrocarbon receptor nuclear translocator (ARNT). AHR/ARNT dimerization forms a transcriptional activator that binds specific DNA enhancer sequences, termed dioxin response elements, to

regulate gene expression (Schmidt and Bradfield, 1996; Rowlands and Gustafsson, 1997). The AHR/ARNT pathway has been extensively studied across vertebrate classes (Hahn, 1998). In fish species, activation of the AHR/ARNT pathway by TCDD along with other members of a large family of related AHR agonists has produced early life stage mortality leading to the near extinction of at least one fish species (Cook et al., 2003).

The best understood target gene for the AHR/ARNT dimer encodes cytochrome P450 1A (CYP1A) (Nebert et al., 1990). In zebrafish embryos exposed shortly after fertilization, TCDD causes a robust and sustained elevation of CYP1A levels (Andreasen et al., 2002b) that precedes development of the different endpoints of toxicity (Henry et al., 1997, Prash et al., 2003). In medaka embryos, TCDD produces elevated CYP1A levels before development of cardiovascular toxicity (Wisk and Cooper, 1990; Cantrell et al., 1996, 1998). Furthermore, in lake trout, the dose-response curves for larval mortality and induction of CYP1A are closely correlated (Guiney

This work was supported by the University of Wisconsin Sea Grant Institute under grants from the National Sea Grant College Program, National Oceanic and Atmospheric Administration, US Department of Commerce, Sea Grant Project Numbers R/BT-16 and R/BT-17 (W.H. and R.E.P.).

ABBREVIATIONS: TCDD, 2,3,7,8-tetrachlorodibenzo-*p*-dioxin; AHR, aryl hydrocarbon receptor; ARNT, aryl hydrocarbon receptor nuclear translocator; MO, morpholino; hpf, hours postfertilization; TBST, Tris-buffered saline/Tween 20; EROD, ethoxyresorufin-O-deethylase; DMSO, dimethyl sulfoxide; mAb, monoclonal antibody; PBS, phosphate-buffered saline; PBST, Phosphate-buffered saline/Tween 20; RBC, red blood cell; zf, zebrafish.

et al., 1997), and the increase in vascular permeability caused by TCDD in trout larvae is preceded by CYP1A mRNA induction (Guiney et al., 2000).

In addition to these correlations, there are several possible mechanisms by which elevated CYP1A could produce developmental toxicity. A widely researched model in fish embryos postulates that increased CYP1A activity could cause oxidative stress by the release of reactive oxygen species from the P450-reductase complex during the activation of molecular oxygen (Schleizinger et al., 2000; Dalton et al., 2002). In support of this model, pretreatment with *N*-acetyl cysteine, an agent that increases glutathione production, provided partial protection against TCDD-induced mortality in medaka (Cantrell et al., 1996) and TCDD-induced reduced blood flow in zebrafish embryos (Dong et al., 2002). In addition, piperonyl butoxide, a compound that inhibits various mixed-function oxidases, also protected against TCDD-induced mortality in medaka embryos (Cantrell et al., 1996). Proadifen and miconazole, other inhibitors of cytochromes P450, also protected against TCDD-induced reductions in mesencephalic vein blood flow in zebrafish embryos (Dong et al., 2002).

These associations between CYP1A induction and toxicity suggest that CYP1A may be the effector enzyme for the AHR/ARNT pathway and that induction of CYP1A may be the mediator of toxic responses in fish embryos. If CYP1A is indeed the mediator of toxic responses, then understanding processes downstream of CYP1A induction is of paramount importance. On the other hand, if CYP1A is not mediating these responses, it will be important to focus on other, as-yet-undiscovered targets for the AHR/ARNT pathway.

The sensitivity of zebrafish embryos to TCDD and the wealth of molecular and genetic tools available with this model organism make the zebrafish an attractive model for examining the mechanism of TCDD toxicity in fish embryos. In the zebrafish, antisense morpholino oligonucleotides (MOs) can be used to knock down expression of specific genes during the early stages of embryonic development (Nasevicius and Ekker, 2000). This enables us to block induction of zfCYP1A by TCDD and determine whether this protects against developmental toxicity. A disadvantage of MO knock-down is that the MO is progressively degraded and diluted until it loses effectiveness around 4 days after fertilization. However, we know that this time frame is sufficient to test the hypothesis, because MO knockdown of zfAHR2, the zebrafish AHR isoform that binds TCDD (Andreasen et al., 2002a), blocked TCDD induction of zfCYP1A and protected against embryotoxicity, demonstrating the role of zfAHR2 in this process (Prasch et al., 2003; Teraoka et al., 2003; Dong et al., 2004).

In this study, we used a *zfcyp1a*-MO to test the hypothesis that zfCYP1A induction causes the toxic responses to TCDD in developing zebrafish. We will show that although the *zfcyp1a*-MO effectively blocked TCDD-induced zfCYP1A protein expression and enzyme activity, it did not protect against TCDD-induced pericardial edema, reduced blood flow, lower jaw malformation, or erythropoiesis defects. Based on these findings, the present publication will conclude that although TCDD causes toxicity through activation of the zfAHR2 signaling pathway, zfCYP1A is not the mediator of these toxic responses.

Materials and Methods

Morpholinos. Morpholinos designed to block initiation of translation of zebrafish aryl hydrocarbon receptor 2 (*zfahr2*-MO) mRNA and zebrafish cytochrome P450 1A (*zfcyp1a*-MO) mRNA were obtained from Gene Tools (Philomath, OR). The *zfahr2*-MO sequence (5'-GTACCGATACCCTCCTACATGGTT-3') complements 24 bases flanking the AUG start codon of zfAHR2 cDNA (GenBank accession number AF063446). The *zfcyp1a*-MO sequence (5'-TGGATACTTTC-CAGTTCTCAGCTCT-3') complements 25 bases of zfCYP1A cDNA (GenBank accession number AB078927) 29 bases upstream from the AUG start codon. Both morpholinos were fluorescein-tagged to monitor injection success. Gene Tools' standard control morpholino (5'-CTCTTACCTCAGTTACAATTTATA-3') was used as the control morpholino (control-MO). The control-MO and *zfcyp1a*-MO were diluted to 0.15 mM and the *zfahr2*-MO to 0.1 mM in Danieau's solution [58 mM NaCl, 0.7 mM KCl, 0.4 mM MgSO₄, 0.6 mM Ca(NO₃)₂, 5 mM HEPES, pH 7.6] before injection (Nasevicius and Ekker, 2000).

Zebrafish Embryos and Microinjection of Morpholinos. Fertilized embryos were obtained from adult AB strain fish bred and maintained in our laboratory at 27°C with a 14-h/10-h light/dark cycle (Westerfield, 1995). Embryos were raised under the same temperature and light conditions in egg water (60 µg/ml Instant Ocean Salts; Aquarium Systems, Mentor, OH) throughout the experiments.

Newly fertilized one-celled embryos were collected at 20-min intervals for microinjection of *zfahr2*-MO, *zfcyp1a*-MO, or control-MO with a Narishige IM300 Microinjector (Tokyo, Japan). Each embryo was injected with 2 nl of morpholino, resulting in about 1.8 ng of *zfahr2*-MO or 2.6 ng of *zfcyp1a*-MO or control-MO delivered to each embryo. Within 2 h of injection, the embryos were sorted to remove unfertilized or damaged embryos. Viable *zfahr2*-MO and *zfcyp1a*-MO-injected embryos were then assessed for fluorescence to determine injection success and even distribution of the morpholino throughout the embryo cell mass. Only *zfahr2*-MO and *zfcyp1a*-MO embryos exhibiting strong fluorescence at 2 h were used.

Waterborne Exposure of Embryos to TCDD. 2,3,7,8-Tetrachlorodibenzo-*p*-dioxin (TCDD) of >99% purity from Chemsyn (Lenexa, KS) was dissolved in dimethyl sulfoxide (DMSO) to prepare a stock solution for dosing. Uninjected embryos, *zfahr2*-MO-injected embryos, *zfcyp1a*-MO-injected embryos, and control-MO-injected embryos were statically exposed to TCDD for 1 h at 4 h postfertilization (hpf) by maintaining embryos in egg water containing either vehicle (0.1% DMSO) or TCDD (0.4 ng/ml). Embryos were placed in glass vials with no more than 3 embryos/ml of egg water and exposed to either vehicle or TCDD for 1 h with gentle rocking. After exposure, the embryos from each vial were rinsed with egg water and transferred to either 1 well of a 24-well plate, 1 well of a six-well plate, or to a 100-mm Petri dish containing egg water.

Experimental Design. Eight treatment groups, uninjected + vehicle, control-MO + vehicle, *zfahr2*-MO + vehicle, *zfcyp1a*-MO + vehicle, uninjected + TCDD, control-MO + TCDD, *zfahr2*-MO + TCDD, and *zfcyp1a*-MO + TCDD, were used in these experiments. For each experiment, *n* was defined as the set of embryos exposed to TCDD or vehicle in a single vial. For the assessment of pericardial edema, red blood cell (RBC) perfusion rate, RBC morphology, and lower jaw morphology, 8 embryos were individually exposed to TCDD or vehicle for each replicate, and *n* = 1 is defined as a single embryo. Two replicates were assessed for pericardial edema, RBC perfusion rate, and lower jaw morphology for a total of *n* = 16 for each treatment group. One replicate with an *n* = 8 for each treatment group was assessed for RBC morphology. For quantitation of zfCYP1A protein, 10 embryos were exposed to TCDD or vehicle in a single vial for each treatment group for each of three replicates. Therefore, *n* = 1 is defined as a set of 10 embryos, and the results of three replicate experiments were averaged. For assessment of zfCYP1A enzyme activity, four embryos were exposed in a single vial for each treatment group. Therefore, *n* = 1 is defined as a group of four embryos, and this experiment was repeated twice. To assess

localization of zfcYP1A protein, three embryos from each treatment group were exposed to TCDD or vehicle. Three replicates were assessed so that $n = 1$ is defined as a set of three embryos, and $n = 3$ for the entire experiment.

Imaging. All observations and imaging were done on a Nikon Eclipse TE300 inverted microscope with epifluorescence and differential interference contrast capabilities. Images and movies were captured using Universal Imaging Corporation Metamorph software and a Princeton Instruments Micromax charge-coupled device camera.

zfcYP1A Protein Abundance. Total zfcYP1A protein in zebrafish embryos from each treatment group was determined by Western blot of protein samples with monoclonal antibody mAb 1-12-3 (Park et al., 1986). Sample embryos were anesthetized (4 mg/ml tricaine), manually deyolked, snap frozen in liquid nitrogen, and stored at -80°C . Protein was extracted from embryos by adding $2\times$ SDS buffer (0.68 M Tris-HCl, pH 6.8, 10% glycerol, 5% β -mercaptoethanol, and 3.5% SDS) to embryos and manually homogenizing tissue. The entire sample for each treatment (10 embryos/lane) was loaded onto an 8% polyacrylamide gel. Samples were transferred to nitrocellulose membranes and blocked 1 h in 5% dry milk in Tris-buffered saline with 0.1% Tween 20 (TBST) before being probed with mouse anti-CYP1A mAb 1-12-3 primary antibody at 0.3 $\mu\text{g}/\text{ml}$, in 1% dry milk in TBST for 1.5 h. After several washes with TBST the membranes were incubated in peroxidase-labeled anti-mouse secondary antibody (1:1000 dilution of stock in 1% dry milk in TBST; ECL Western Blotting analysis system, Amersham Biosciences) for 2 h then washed again several times in TBST. Protein bands for zfcYP1A were visualized by addition of ECF reagent (ECF Western Blotting Analysis System, Amersham Biosciences) to the membranes followed by chemiluminescence detection using a Storm PhosphorImager (Amersham Biosciences). Individual bands in the captured images were quantitated in ImageQuant.

Ethoxyresorufin O-deethylase Assay. To assess zfcYP1A enzyme activity in embryos from each treatment group, an *in vivo* EROD assay was performed in which nonfluorescent 7-ethoxyresorufin diffuses into the embryo and is O-deethylated to a fluorescent product, resorufin, by zfcYP1A (Nacci et al., 1998). 7-Ethoxyresorufin (Sigma) was dissolved in DMSO to prepare a stock solution (0.8 mg/ml). Individual embryos from each treatment group were exposed to 0.4 $\mu\text{g}/\text{ml}$ ethoxyresorufin for 5 min by adding the appropriate volume of stock solution to embryos in egg water. At the end of the incubation period, embryos were mounted in 3% methylcellulose to immobilize the embryos for observation and imaging with epifluorescence microscopy equipped with an EROD filter (excitation λ , 577 nm; emission λ , 620 nm).

Whole-Mount Immunolocalization of zfcYP1A. Tissue-specific expression of zfcYP1A in zebrafish embryos from each treatment group was determined using monoclonal antibody mAb 1-12-3 as described previously (Andreasen et al., 2002b; Prasch et al., 2003). In brief, embryos were fixed overnight in 4% paraformaldehyde in phosphate-buffered saline (PBS) at 4°C , dehydrated in a methanol series, and stored at -20°C for several days. Embryos were rehydrated gradually into PBS, incubated 20 min in acetone at -20°C , washed once with PBS, and then digested in collagenase (1 mg/ml) for 45 min to permeabilize embryos for staining. Embryos were then blocked in 10% normal calf serum in PBS with 0.1% Tween 20 (PBST) for 1 h followed by an overnight incubation at 4°C in 0.3 $\mu\text{g}/\text{ml}$ mAb 1-12-3. After being washed several times in PBST, embryos were incubated with a secondary antibody (Alexa-488 conjugated goat anti-mouse; Molecular Probes, Eugene, OR) for 5 h at room temperature. Embryos were washed several times with PBST and stored in glycerol at 4°C for 48 h before visualization by epifluorescence microscopy. To control for nonspecific staining by the secondary antibody, a subset of embryos was stained without addition of the primary mAb 1-12-3 antibody, and no staining was observed in these embryos.

Pericardial Sac Area. The incidence and amount of pericardial edema in embryos from each treatment group were determined by quantitation of the pericardial sac area. Embryos were mounted in 3% methylcellulose, carefully positioned for imaging of the lateral view, and photographed. To measure pericardial sac area, the pericardial sac of each lateral view image was outlined, and the area within each outline quantitated by Scion Image for Windows (<http://www.scioncorp.com>). The average pericardial area in vehicle-treated uninjected embryos without edema was calculated as background and subtracted from each measurement; the resulting value represents the area due to edema caused by the treatment applied to each group.

Red Blood Cell Perfusion Rate. As an index of regional blood flow in the trunk, the RBC perfusion rate was measured in an intersegmental vessel in the posterior quarter of the trunk as first described by Teraoka et al. (2002). Time-lapse recordings of embryos mounted in 3% methylcellulose were used to image RBCs passing through an intersegmental vessel in 10 s as described by Prasch et al. (2003). In brief, RBCs were recorded for 100 frames (10 s), and the stacks of images were converted to movies with Metamorph software so that the number of RBCs passing a defined point in the intersegmental vessel could be counted.

Lower Jaw Morphology. To assess lower jaw morphology, embryos from each treatment group were mounted in 3% methylcellulose, carefully positioned for imaging of the lateral view of the head, and photographed. The distance of the gap between the anterior edge of the eye and the posterior end of Meckel's cartilage was determined and used as an index of lower jaw extension.

Erythrocyte Morphology. Blood collection and determination of RBC shape were performed as described previously (Belair et al., 2001; Prasch et al., 2003). In brief, RBCs were collected from anesthetized zebrafish embryos (4 mg/ml tricaine in 1% bovine serum albumin in calcium and magnesium-free PBS, pH 7.4) from each treatment group onto glass slides by cardiac puncture. The RBCs were observed by differential interference contrast microscopy and photographed. The number of round and elliptical RBCs from each embryo was counted to calculate the percentage that each cell type contributed to the total.

Statistical Analysis. Significance was determined for all endpoints, except 72 hpf pericardial edema and zfcYP1A protein quantitation, using a two-way analysis of variance followed by the Fisher least significant difference post hoc test. Untransformed data sets that did not pass Levene's test for homogeneity of variances were transformed by \log_{10} transformation (RBC morphology) or inverse transformation (96 hpf pericardial edema) before analysis by two-way analysis of variance followed by the Fischer least significant difference post hoc test. All attempts to transform the 72 hpf pericardial edema data set and Western blot quantitations to pass Levene's test failed. Therefore, significance between appropriate treatment groups was determined by individual *t* tests assuming unequal variance. Statistica 6.0 software (StatSoft, Inc., Tulsa, OK) was used to perform all statistical analyses. Results are presented as mean \pm S.E.; level of significance was $p \leq 0.05$.

Results

MO Knockdown of zfcYP1A Protein Levels in Zebrafish Embryos Exposed to TCDD. When newly fertilized zebrafish embryos are exposed to TCDD, *zfcyp1a* transcription is strongly induced following a time course that coincides with the developmental window in which embryos are most sensitive to TCDD toxicity (Prasch et al., 2003). This is demonstrated in Western blots measuring zfcYP1A protein levels at 48, 72, and 96 hpf in zebrafish embryos exposed to TCDD shortly after fertilization (Fig. 1). Increased zfcYP1A expression precedes the development of toxic responses to TCDD, including pericardial edema, reduced blood

flow, reduced lower jaw growth, and a block in erythropoiesis (Henry et al., 1997; Belair et al., 2001; Teraoka et al., 2002; Prasch et al., 2003). The early onset of increased *zfcyp1a* expression, coupled with the fact that CYP1A is the most well known target for the AHR/ARNT pathway, raises the possibility that transcriptional activation of *zfcyp1a* may be the proximate cause of TCDD developmental toxicity.

We have shown previously that most, if not all, of the endpoints of TCDD developmental toxicity in zebrafish are

dependent on TCDD activation of the AHR/ARNT pathway (Prasch et al., 2003). MO knockdown of *zfAHR2* expression is sufficient to protect developing zebrafish from TCDD toxicity throughout the normal length of MO effectiveness, from approximately 0 to 72 hpf. If *zfcyp1a* is the downstream effector for AHR/ARNT mediated toxicity, then knockdown of *zfcyp1a* expression should also block TCDD toxicity. Western blots of *zfcyp1a* protein at 48, 72, and 96 hpf in *zfcyp1a* morphants treated with TCDD, or vehicle as a control, confirmed the effectiveness of the *zfcyp1a*-MO in blocking the increased levels of *zfcyp1a* produced by TCDD (Fig. 1). As expected (Prasch et al., 2003; Teraoka et al., 2003), MO knockdown of *zfAHR2* also blocked *zfcyp1a* protein induction. In embryos injected with a control-MO, the TCDD induction of *zfcyp1a* protein at 48, 72, and 96 hpf was the same as that observed in uninjected embryos, demonstrating the specificity of the MOs.

Both the *zfahr2*- and *zfcyp1a*-MOs effectively inhibited induction of CYP1A protein throughout the 96-h time course of the experiment. However, at later time points, TCDD produced a small but significant increase in *zfcyp1a* protein levels, even in the *zfahr2*-MO- and *zfcyp1a*-MO-treated embryos (Fig. 1). This is very probably caused by progressive dilution and loss of effectiveness of the MO with time. Regardless, both MOs produced significant reduction in *zfcyp1a* levels, and the *zfcyp1a*-MO was at least as effective as the *zfahr2*-MO in reducing *zfcyp1a* protein levels.

An *in vivo* assay of *zfcyp1a* enzyme activity confirmed that both the *zfahr2*- and *zfcyp1a*-MOs effectively block induction of *zfcyp1a* by TCDD (Fig. 2). In this assay, *O*-deethylation of ethoxyresorufin (EROD activity) by *zfcyp1a* produces a fluorescent product, resorufin. Therefore, increased fluorescence in the embryo marks an increase in *zfcyp1a* enzyme activity. Figure 2 shows representative embryos at 48, 72, and 96 hpf exposed to vehicle or TCDD as well as a *zfahr2* morphant and a *zfcyp1a* morphant exposed to TCDD. At 48 and 72 hpf, TCDD-treated embryos have clearly elevated EROD fluorescence compared with vehicle-treated embryos. In marked contrast, the *zfahr2* and *zfcyp1a* morphants exposed to TCDD exhibited only slightly more fluorescence than vehicle-exposed embryos. Consistent with the Western blot results, by 96 hpf, the *zfahr2* and *zfcyp1a* morphants exposed to TCDD had higher levels of fluorescence than control, untreated embryos, but this remained well below that of the uninjected and control-MO-injected embryos exposed to TCDD. These results demonstrate MO knockdown of *zfcyp1a* enzyme induction by both *zfahr2*-MO and *zfcyp1a*-MO.

Whole mount immunolocalization of *zfcyp1a* using the mAb 1-12-3 antibody revealed that the *zfahr2*-MO and *zfcyp1a*-MO both blocked TCDD-induced *zfcyp1a* throughout the embryo tissues. Figure 3 shows representative embryos exposed to vehicle or TCDD shortly after fertilization and collected for whole mount immunolocalization at 72 hpf. Fig. 3, left, shows *zfcyp1a* immunostaining in the trunk region posterior to the anal pore and on the right in the head region. Very little staining occurred in vehicle-treated embryos: weak levels of *zfcyp1a* immunofluorescence were observed in some intersegmental vessels, the caudal artery and vein, and the branchial arches of the jaw, but no staining was observed in the head. In contrast, embryos exposed to TCDD showed strong *zfcyp1a* immunofluorescence in the interseg-

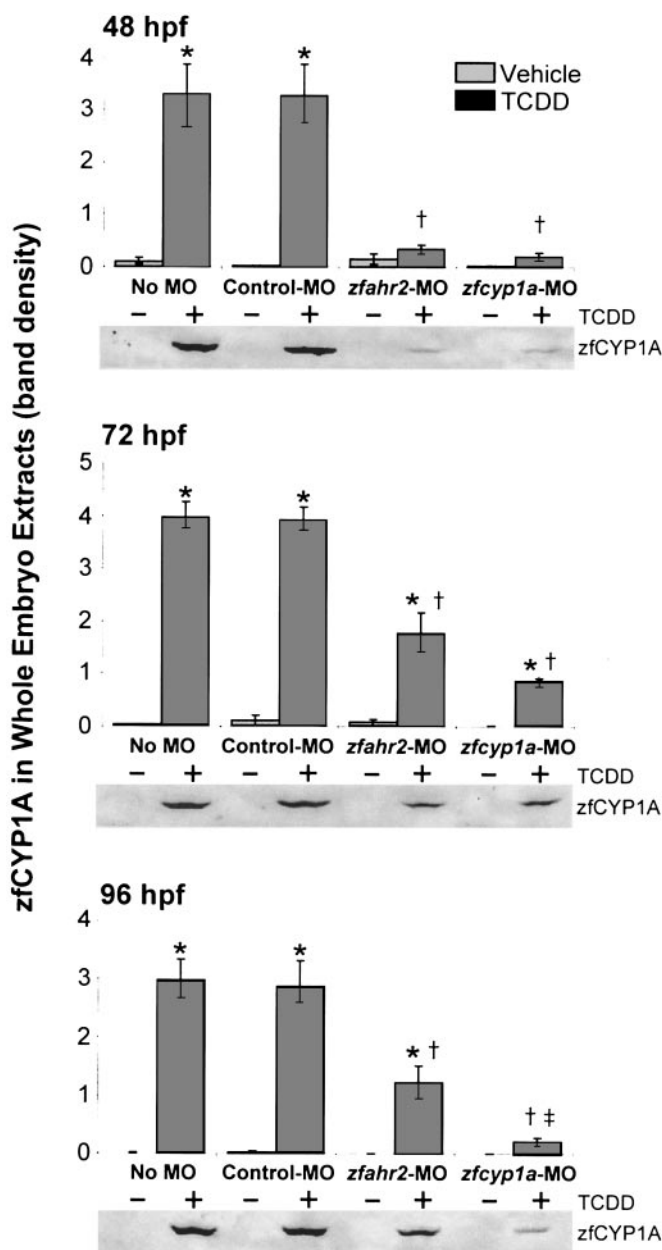


Fig. 1. Effect of *zfahr2*-MO and *zfcyp1a*-MO in blocking TCDD-induced increase in *zfcyp1a* protein expression from 48 to 96 hpf in zebrafish embryos. Western blots of protein extracted from each treatment group at 48, 72, and 96 hpf were performed using mAb 1-12-3 to detect *zfcyp1a* protein. Protein bands from three replicate blots were quantitated and graphed as the abundance of *zfcyp1a*. Values are mean \pm S.E. of $n = 3$. *, significant difference between TCDD (0.4 ng/ml) and its respective vehicle control for each treatment. †, significant difference between TCDD and TCDD + morpholino. ‡, significant difference between TCDD + *zfahr2*-MO and TCDD + *zfcyp1a*-MO ($p < 0.05$). Representative blots are shown for each of the three time points.

mental vessels, caudal artery, caudal vein, brain vessels throughout the head, and the anal and urinary pores. Staining was also evident in the branchial arches (ba) of the lower jaw. *Zfah2* morphants exposed to TCDD showed only weak zfcyp1a immunofluorescence in the intersegmental vessels, caudal artery, caudal vein, brain vessels, and branchial arches of the lower jaw. There was no visible staining in the anal and urinary pores. *Zfcyp1a* morphants exposed to TCDD also showed weak zfcyp1a immunostaining in the trunk vessels (intersegmental vessel, caudal artery, caudal vein) but not in the anal or urinary pores. Staining in the brain vessels was very weak, and there was also weak staining in the branchial arches of the jaw. Overall, the staining in the *zfah2*-MO and *zfcyp1a*-MO-treated embryos was comparable with the staining in the vehicle-treated embryos.

Morpholino Knockdown of zfcyp1a Protein Levels Fails to Block Toxic Responses to TCDD. The experiments described above demonstrate the effectiveness of the *zfcyp1a*-MO in blocking induction of zfcyp1a by TCDD. As described above, the knockdown was not complete at later time points. However the *zfah2*-MO has been shown to block TCDD toxicity in early life stage zebrafish (Prasch et al., 2003). If CYP1A mediates the toxicity, then the degree of reduction in zfcyp1a levels produced by the *zfah2*-MO must be sufficient to alleviate toxicity. In this case, the *zfcyp1a*-MO should be equally effective as the *zfah2*-MO in preventing these toxic responses. However, we found that this was not the case.

Edema is a classic sign of TCDD exposure in zebrafish embryos, it starts to develop around 72 hpf and increases in severity until mortality occurs around 8 to 10 days after fertilization (Henry et al., 1997). The *zfah2*-MO has previously been shown to protect against TCDD-induced pericardial edema in zebrafish embryos (Prasch et al., 2003; Teraoka et al., 2003). We measured pericardial sac area in embryos from each treatment group to determine the ability of the *zfcyp1a*-MO to protect against TCDD-induced pericardial edema (Fig. 4). TCDD exposure caused a significant accumulation of pericardial edema fluid in uninjected zebrafish embryos by 72 hpf that was increased in severity by 96 hpf. Injection of embryos with a control-MO did not alter this response to TCDD. The mean pericardial edema in 96 hpf uninjected embryos exposed to TCDD is slightly, but not significantly, elevated above the mean pericardial edema in

control morphants and *zfcyp1a* morphants exposed to TCDD. This slight difference in means is the result of two uninjected embryos exposed to TCDD that developed fairly severe pericardial edema by 96 hpf, not a nonspecific effect from treatment with morpholino that reduced the severity of pericardial edema induced by TCDD. As in earlier work, injection of *zfah2*-MO effectively protected against the increase in pericardial sac area caused by TCDD. In marked contrast to the *zfah2*-MO, the *zfcyp1a*-MO did not prevent the increase in pericardial sac area caused by exposure to TCDD, and pericardial edema in *zfcyp1a* morphants was no less severe than that in control morphants exposed to TCDD. Figure 4 shows representative photographs of edema in the pericardial sac (ps) in 96 hpf embryos exposed to TCDD or vehicle, the protection afforded against pericardial edema by the *zfah2*-MO-injected into embryos before TCDD exposure, and the lack of protection against pericardial edema in control morphants and *zfcyp1a* morphants treated with TCDD.

Circulation failure in developing zebrafish exposed to TCDD is first observed by reduced blood flow in the trunk vasculature between 60 and 72 hpf, followed by reductions in blood flow in the head vessels, and ultimately by cessation of flow throughout the embryo by 96 to 144 hpf (Henry et al., 1997; Prasch et al., 2003; Teraoka et al., 2003). Embryos injected with *zfah2*-MO are protected against TCDD-induced reductions in blood flow through 120 hpf (Prasch et al., 2003). To determine whether the protection against TCDD-induced reductions in blood flow afforded by the *zfah2*-MO is caused by decreases in zfcyp1a, RBC perfusion rates in the trunk intersegmental vessels posterior to the anal pore were measured at 72 and 96 hpf in control morphants, *zfah2* morphants, *zfcyp1a* morphants, and uninjected embryos exposed to TCDD or vehicle (Fig. 5). At 72 hpf, TCDD reduced RBC perfusion in uninjected embryos and control morphants by more than 50%. As shown in earlier work, *zfah2* morphants treated with TCDD did not have significantly reduced RBC perfusion. Unlike *zfah2* morphants, *zfcyp1a* morphants exposed to TCDD showed a reduction in RBC perfusion by more than 50% that was not significantly different from control morphants treated with TCDD. By 96 hpf, uninjected embryos and control morphants treated with TCDD had almost no blood flow in the intersegmental trunk vessels. The *zfah2*-MO completely protected against this reduction in RBC perfusion in the intersegmental vessels caused by

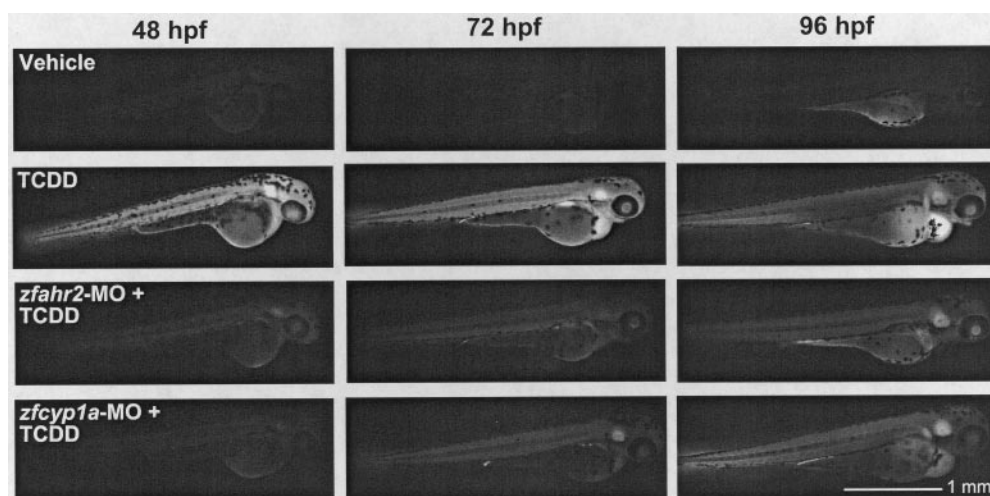


Fig. 2. Effect of *zfah2*-MO and *zfcyp1a*-MO on TCDD-induced increase in zfcyp1a enzyme activity from 48 to 96 hpf in zebrafish embryos. An in vivo EROD assay was performed on embryos from each treatment group at 48, 72, and 96 hpf to assess the effectiveness of the *zfah2*-MO and *zfcyp1a*-MO in blocking TCDD-induced zfcyp1a enzyme activity. Representative vehicle-exposed, TCDD-exposed (0.4 ng/ml), TCDD-exposed embryos injected with *zfah2*-MO, and TCDD-exposed embryos injected with *zfcyp1a*-MO from four embryos from three different vehicle/TCDD exposures are shown. Scale bar, 1 mm.

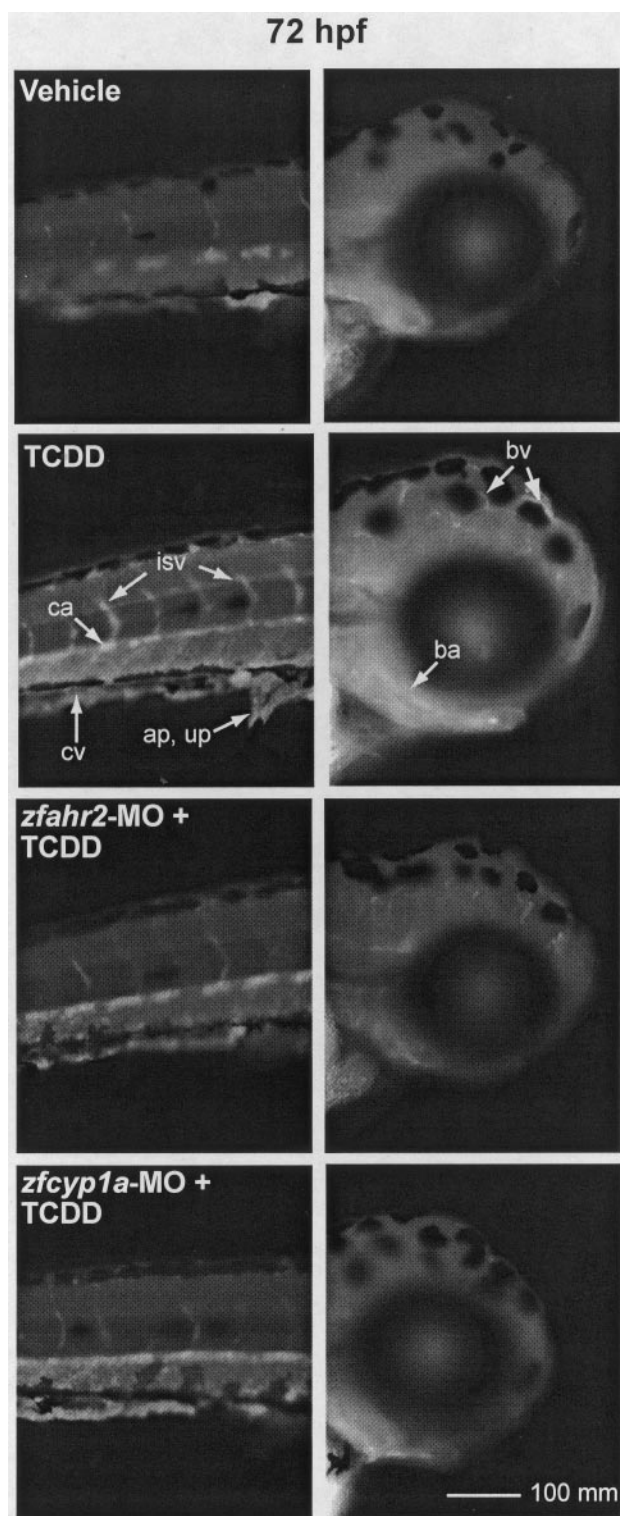


Fig. 3. Whole mount immunolocalization of zfCYP1A in 72 hpf zebrafish embryos using mAb 1-12-3. Immunohistochemistry to determine the effectiveness of the *zfahr2*-MO and *zfcyp1a*-MO in blocking TCDD-induced zfCYP1A protein throughout the embryo was performed on embryos from each treatment group. Representative vehicle-exposed, TCDD-exposed (0.4 ng/ml), TCDD-exposed embryos injected with *zfahr2*-MO, and TCDD-exposed embryos injected with *zfcyp1a*-MO from nine embryos from three different vehicle/TCDD exposures are shown. Images on the left are lateral views of the trunk just posterior to the yolk extension, and images on the right are lateral views of the head just anterior to the yolk sac. ap, anal pore; bv, brain vessels; ba, brachial arches; ca, caudal artery; cv, caudal vein; isv, intersegmental vessel; up, urinary pore. Scale bar, 100 μ m.

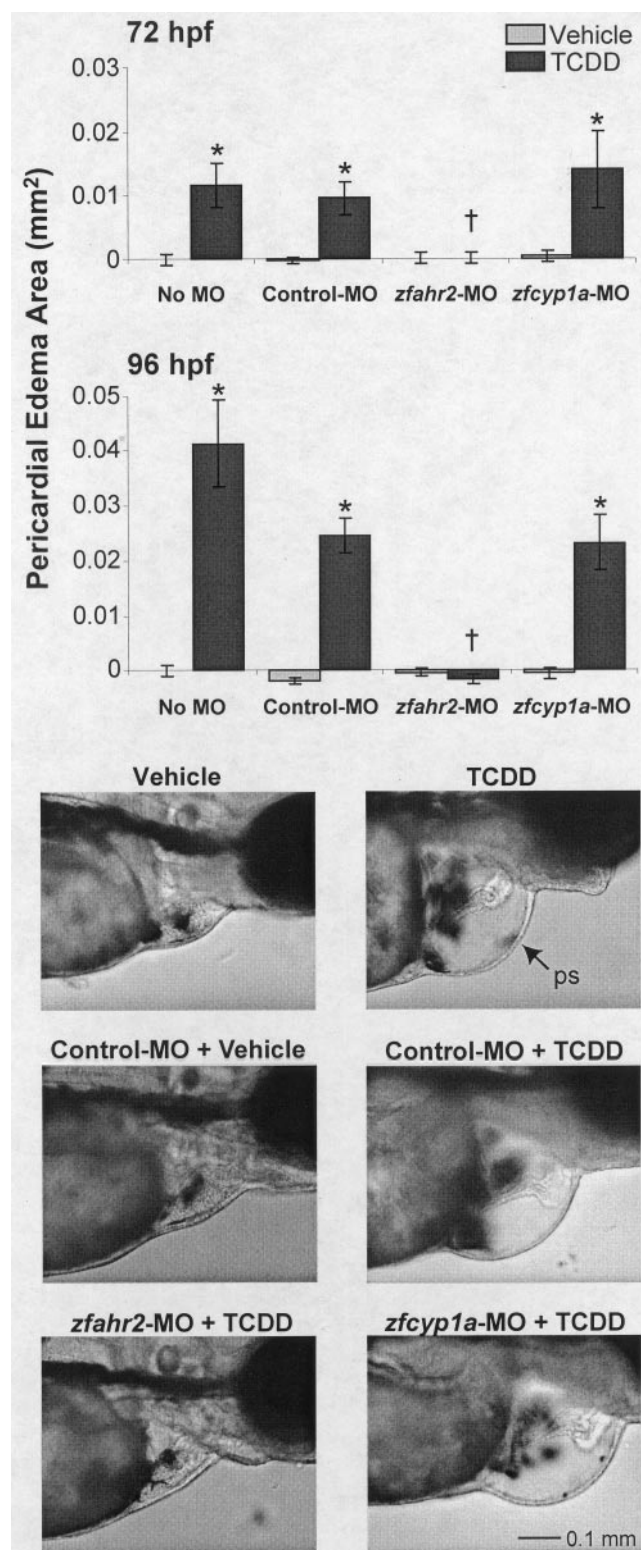


Fig. 4. Effect of *zfahr2*-MO and *zfcyp1a*-MO on TCDD-induced pericardial sac area caused by edema in zebrafish embryos. Lateral view images of embryos from all treatment groups were photographed and the pericardial edema quantitated at 72 and 96 hpf from measurements of the pericardial sac (ps) area. Images on the bottom are representative photos of pericardial edema at 96 hpf in uninjected embryos exposed to vehicle or TCDD, control morphants exposed to vehicle or TCDD, *zfahr2* morphants exposed to TCDD, and *zfcyp1a* morphants exposed to TCDD. Values are mean \pm S.E. of $n = 16$. *, significant difference between TCDD (0.4 ng/ml) and its respective vehicle control for each treatment. †, significant difference between TCDD and TCDD + morpholino ($p < 0.05$). Scale bar, 0.1 mm.

TCDD. In contrast to the *zfahr2* morphants, intersegmental blood flow in *zfcyp1a* morphants exposed to TCDD had practically ceased by 96 hpf, and could not be distinguished from the flow rate in uninjected embryos exposed to TCDD.

TCDD exposure of zebrafish embryos retards growth in the cartilaginous structures of the jaw resulting in malformation (Teraoka et al., 2002). One of the most pronounced effects of this malformation is the failure of Meckel's cartilage in the lower jaw to extend beyond the eye by 120 hpf. The *zfahr2*-MO protects against TCDD-induced inhibition of lower jaw growth (Prasch et al., 2003). However, this protection is transient, lasting only as long as the morpholino remains at levels that effectively block translation of *zfAHR2* and signaling through the AHR/ARNT pathway. We measured the distance between the tip of Meckel's cartilage and the anterior edge of the eye, the "lower jaw-to-eye gap," in 96 hpf zebrafish to determine whether blocking *zfCYP1A* induction would protect against the retarded lower jaw growth produced by TCDD (Fig. 6). Uninjected embryos and control morphants exposed to TCDD have a lower jaw-to-eye gap at least twice as great as that measured in vehicle-treated embryos, indicating a significant reduction in lower jaw growth. Injection of embryos with *zfahr2*-MO before TCDD exposure leads to significant protection against the reduction in lower

jaw growth, as seen in earlier work. Unlike the *zfahr2*-MO, injection of embryos with *zfcyp1a*-MO before TCDD exposure does not protect against the reduction in lower jaw growth. The lower jaw-to-eye gap in *zfcyp1a* morphants exposed to

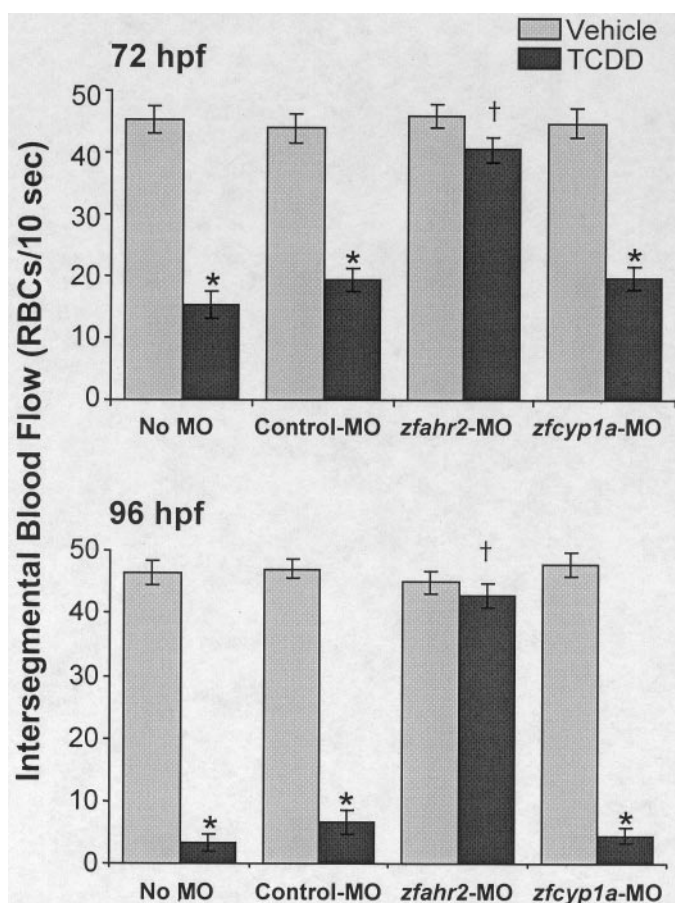


Fig. 5. Effect of *zfahr2*-MO and *zfcyp1a*-MO on TCDD-induced reductions in RBC perfusion rate caused by decreased blood flow in zebrafish embryos. RBC perfusion rates were determined in an intersegmental vessel posterior to the anal pore in embryos from each treatment at 72 and 96 hpf. Values are mean \pm S.E. of $n = 16$. *, significant difference between TCDD (0.4 ng/ml) and its respective vehicle control for each treatment. †, significant difference between TCDD and TCDD + morpholino ($p < 0.05$).

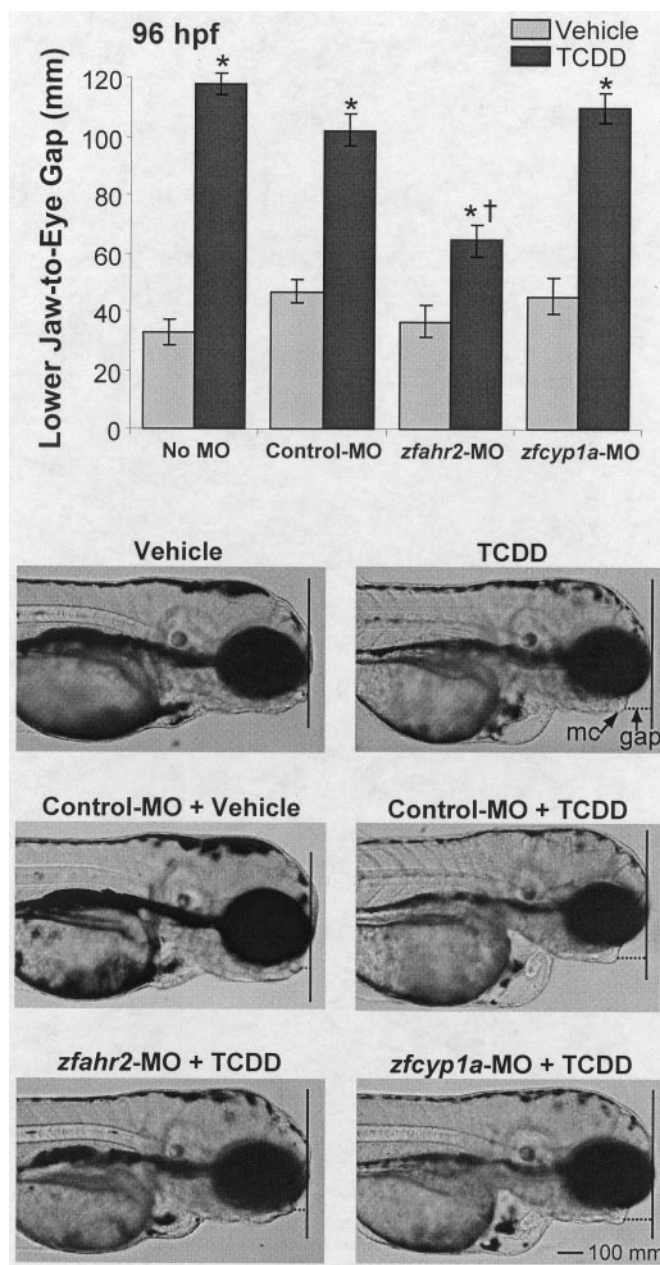


Fig. 6. Effect of *zfahr2*-MO and *zfcyp1a*-MO on TCDD-induced alterations in lower jaw morphology in zebrafish embryos. Lateral view images of embryos from all treatment groups were photographed at 96 hpf to determine the lower jaw-to-eye gap. To measure the distance between the anterior edge of the eye and the posterior end of Meckel's cartilage (mc), a vertical solid line was drawn at the anterior edge of the eye, and a horizontal dashed line was drawn between the solid line and the anterior tip of Meckel's cartilage. The length of the dashed line, or the distance between Meckel's cartilage and the anterior edge of the eye, is the lower jaw-to-eye gap. Values are mean \pm S.E. of $n = 16$. *, significant difference between TCDD (0.4 ng/ml) and its respective vehicle control for each treatment. †, significant difference between TCDD and TCDD + morpholino ($p < 0.05$). Images on the bottom are representative photos of the extension of the lower jaw in uninjected embryos exposed to vehicle or TCDD, control morphants exposed to vehicle or TCDD, *zfahr2* morphants exposed to TCDD, and *zfcyp1a* morphants exposed to TCDD. Scale bar, 100 μ m.

TCDD is not significantly different from control morphants exposed to TCDD.

Figure 6 also shows representative photographs illustrating the increased lower jaw-to-eye gap in TCDD-treated embryos as a measure of reduced lower jaw growth. Meckel's cartilage (mc) extends almost to the anterior edge of the eye in vehicle-treated embryos at 96 hpf, whereas in TCDD-treated embryos, the cartilage extends just beyond the midpoint of the eye. In *zfahr2* morphants exposed to TCDD, Meckel's cartilage extends well past the midpoint of the eye but does not quite reach the anterior edge of the eye. TCDD reduces lower jaw growth in control morphants and *zfcyp1a* morphants so that Meckel's cartilage extends only just beyond the midpoint of the eye as observed in uninjected embryos exposed to TCDD.

TCDD causes anemia in zebrafish embryos by blocking the switch from primitive to definitive erythropoiesis (Belair et al., 2001). The first wave of erythropoiesis produces round primitive RBCs. By 120 hpf, the adult form of erythrocytes, elliptical RBCs resulting from definitive erythropoiesis, start appearing in the circulating blood. Over the next 48 h, the percentage of round RBCs drops and elliptical cells eventually make up the entire RBC population. In zebrafish embryos, this transition from round to elliptical RBCs is blocked when embryos are exposed to TCDD before 96 hpf (Belair et al., 2001). This indicates that the developmental signal for the switch from primitive to definitive erythropoiesis that is disrupted by TCDD occurs within the developmental window in which both the *zfahr2*-MO and *zfcyp1a*-MO effectively block the TCDD induction of *zfcyp1a*. Prasch et al. (2003) showed that the *zfahr2*-MO effectively protects against this TCDD-induced block of definitive erythropoiesis, indicating this endpoint of TCDD toxicity is mediated by *zFAHR2*. To determine whether this protection by the *zfahr2*-MO is caused by its ability to block TCDD-induced *zfcyp1a* expression, we examined the morphology of the RBCs in *zfcyp1a* morphants treated with TCDD (Fig. 7). At 144 hpf, adult elliptical erythrocytes made up approximately 90% of RBCs

in vehicle-treated zebrafish, whereas only 30% of RBCs were elliptical in TCDD-treated embryos. In *zfahr2* morphants, the effect of TCDD was blocked and approximately 80 to 90% of the erythrocytes were elliptical, as in vehicle-treated embryos. In contrast, *zfcyp1a* morphants had an erythrocyte profile similar to that of uninjected or control morphants; adult elliptical cells comprised only 30% of the RBCs in TCDD-exposed embryos.

Discussion

Morphants, *zfcyp1a* Protein Expression, and TCDD Developmental Toxicity. In this study, we blocked translation of *zfcyp1a* in TCDD-treated zebrafish embryos to determine whether *zfcyp1a* mediates developmental toxicity. We initiated these experiments knowing that the MO knockdown approach is capable of blocking toxic responses to TCDD in developing zebrafish. Three previous studies showed that MO knockdown of *zFAHR2* during embryonic development prevents signs of TCDD toxicity (Dong et al., 2004; Prasch et al., 2003; Teraoka et al., 2003). Our results confirm the previous experiments showing that *zFAHR2* mediates TCDD induction of both *zfcyp1a* expression and developmental toxicity. However, our experiments clearly dissociate *zfcyp1a* induction by TCDD from these toxic responses.

The *zfahr2*-MO completely prevented TCDD-induced pericardial edema, reduced blood flow, and defects in erythropoiesis. The *zfahr2*-MO also significantly, but not completely, protected embryos against TCDD-induced lower jaw malformations, and produced substantial reductions in *zfcyp1a* induction by TCDD. In contrast, although the *zfcyp1a*-MO was at least as effective in preventing TCDD-induced *zfcyp1a* expression, the *zfcyp1a*-MO had no observable impact on TCDD-induced toxic responses. Therefore, the *zfahr2*-MO cannot have prevented toxicity by blocking *zfcyp1a* induction, and CYP1A cannot be the downstream effector mediating the toxic responses of AHR/ARNT pathway activation examined in this study.

This result came as some surprise because an earlier study by Teraoka et al. (2003) indicated that the *zfcyp1a*-MO could protect against TCDD-induced pericardial edema and reduced intersegmental blood flow. Because our results are at odds with the previously published work, we have been extremely careful to demonstrate the reproducibility of our results, and to use several different approaches to prove that the *zfcyp1a*-MO does indeed knock down *zfcyp1a* expression induced by TCDD. We found two very consistent results. First, the *zfcyp1a*-MO was always at least as effective as the *zfahr2*-MO in reducing *zfcyp1a* induction by TCDD. Second, in contrast to the *zfahr2*-MO, the *zfcyp1a*-MO consistently had no effect on the signs of TCDD-induced toxicity that we measured. We used the same *zfcyp1a*-MO sequence as in the previous report, and at present cannot explain the discrepancy in the results. We do note, however, that the assays published by Teraoka et al. (2003) examined toxicity only in 72 hpf embryos. In our hands, 72 hpf is near the earliest onset for these endpoints, especially with lower doses of TCDD. At this time, the signs of TCDD toxicity are subtle, and it is possible to mistake small responses for a lack of response. In our experiments we examined embryos at 72 hpf and also at 96 hpf, a point at which the MOs are still effective and the responses to TCDD are quite robust. Despite the

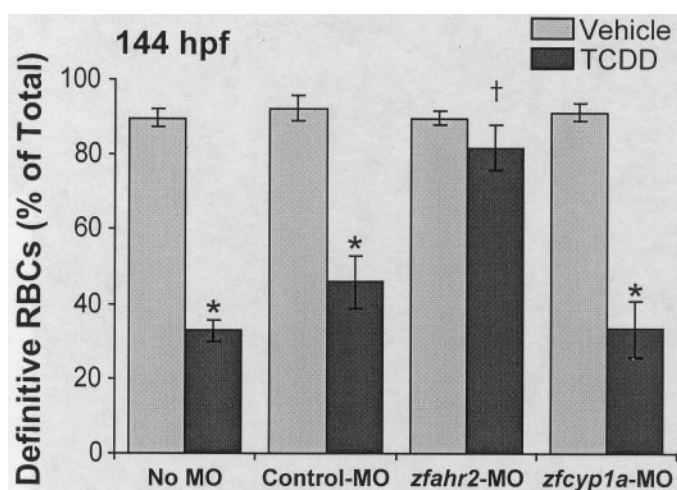


Fig. 7. Effect of *zfahr2*-MO and *zfcyp1a*-MO on TCDD-induced block of definitive erythropoiesis in zebrafish embryos. RBCs collected from embryos from each treatment group at 144 hpf were classified as either primitive round erythrocytes or definitive elliptical erythrocytes. Alterations in the percentage of elliptical RBCs are shown. Values are mean \pm S.E. of $n = 8$. *, significant difference between TCDD (0.4 ng/ml) and its respective vehicle control for each treatment. †, significant difference between TCDD and TCDD + morpholino ($p < 0.05$).

extension of our study to a later time point and investigation of additional endpoints of toxicity induced by TCDD activation of zfAHR2, we found no evidence that zfCYP1A induction mediates developmental toxicity in zebrafish.

Our *zfcyp1a*-MO was specifically directed against *zfcyp1a*. Therefore we cannot rule out the possibility that TCDD induces other zebrafish P450 enzymes to produce toxicity. Unlike mammals, fish species do not seem to have orthologues of *cyp1a1* and *cyp1a2*, but rather have a single *cyp1a* gene that presumably corresponds to the ancestral gene that diverged into *cyp1a1* and *cyp1a2* in mammals (Morrison et al., 1998). However, other isoforms of *cyp1a* may have arisen from further genome duplications during teleost evolution. Our BLAST searches of the zebrafish genome have not revealed other *cyp1a* isoforms. If such an isoform exists and can be induced by TCDD, it does not have the properties normally associated with CYP1A. That is, it does not *O*-deethylate ethoxyresorufin, nor does it immunoreact with mAb 1-12-3, an antibody that reacts with CYP1A proteins in many species (Borlakoglu et al., 1991; Drahushuk et al., 1998; Huang et al., 2001; Hyyti et al., 2001). Because TCDD-induced EROD activity and immunoreactivity with mAb 1-12-3 was reduced by *zfcyp1a*-MO injection to levels near those observed in vehicle-treated embryos it seems unlikely that TCDD causes toxicity through the induction of another isoform of *cyp1a*.

Our results are consistent with findings in mammalian systems suggesting that although CYP1A mediates some responses to TCDD, it is not the conduit through which all TCDD responses are initiated. Female *cyp1a1*-null mice exposed to TCDD have some protection against thymus and splenic atrophy (Uno et al., 2002). Disruption of *cyp1a2* in mice protected against TCDD-induced uroporphyrin and some hepatocellular damage (Smith et al., 2001), but other signs of toxicity were not prevented. Any protection afforded *cyp1a1*- or *cyp1a2*-null mice exposed to TCDD during embryonic development has not been reported. In rat lines selectively bred for varying sensitivity to TCDD toxicity, induction of *cyp1a* has been dissociated from many of the overt toxic responses to TCDD. These rat lines have differences in sensitivity to TCDD toxicity of several orders of magnitude yet have TCDD ED₅₀ values for EROD induction that are not significantly different (Tuomisto et al., 1999; Simanainen et al., 2003), suggesting that there is no correlation between CYP1A activity and certain endpoints of TCDD toxicity. In addition, a study by Hakansson et al. (1994) found no correlation between hepatic EROD activity induced by TCDD and various endpoints of toxicity in several rodent species, including Hartley guinea pigs and Golden Syrian hamsters. Although it is likely that TCDD-up-regulated CYP1A-metabolizing enzymes contribute in some way to the progression of toxicity in mammals, the degree of protection will probably be species-, tissue-, gender-, and life stage-specific. Unlike mammals, TCDD up-regulation of CYP1A in fish embryos is spatially associated, and in some cases well correlated, with endpoints of developmental toxicity (Guiney et al., 1997; Cantrell et al., 1998; Toomey et al., 2001; Andreassen et al., 2002b; Dong et al., 2002; Prasch et al., 2003). In addition, Schlezinger et al. (2000) reported that another halogenated aromatic hydrocarbon AHR agonist, 3,3',4,4'-tetrachlorobiphenyl, stimulates reactive oxygen species production both in fish and mammalian liver microsomes, suggesting that 3,3',4,4'-tetrachlorobiphenyl uncouples electron transfer

events within the CYP1A complex. It has been postulated that generation of reactive oxygen species by CYP1A uncoupling may cause oxidative stress and contribute to the developmental toxicity in fish embryos caused by TCDD and other halogenated aromatic hydrocarbons.

Despite the evidence suggesting a role for CYP1A in mediating TCDD developmental toxicity in fish investigated through the use of cytochrome P450 inhibitors and compounds that protect against oxidative stress (Cantrell et al., 1996; Dong et al., 2002), TCDD induction of *zfcyp1a* does not mediate developmental toxicity in zebrafish embryos in the present study. Although our experiments show that induction of *zfcyp1a* by TCDD does not play a role in mediating endpoints of developmental toxicity in zebrafish, induction of *zfcyp1a* in zebrafish may be important in mediating TCDD toxicity during later life stages of zebrafish or in mediating toxicity of other AHR agonists. The results of this study also do not rule out the possibility that oxidative stress has a role in mediating TCDD developmental toxicity in zebrafish, but one of the most significant aspects of our work is that it directs our attention away from events downstream of *zfcyp1a* induction and focuses our efforts on examining other mechanisms of TCDD toxicity.

CYP1A-Independent Mechanisms of TCDD Toxicity.

Since the initial identification of the AHR gene battery (Nebert et al., 1990; Rowlands and Gustafsson, 1997), research with various cell systems and model organisms has revealed that TCDD alters expression of numerous genes with a wide range of cellular functions (Fisher et al., 1990; Puga et al., 2000; Frueh et al., 2001). The large number of genes activated by TCDD, and the growing list of genes known to have upstream dioxin response elements, support a model in which TCDD toxicity results from persistent misregulation of genes controlled by the AHR/ARNT complex.

It also should be noted that the possible mechanisms extend beyond altered transcription of genes directly regulated by AHR/ARNT. A recent review by Carlson and Perdew (2002) outlines cross-talk between components of the AHR/ARNT transcriptional complex and regulation of genes by steroid hormone receptor complexes, hypoxia inducible factor-1 α , nuclear factor κ B, as well as retinoblastoma and other cell cycle proteins. These interactions affect both transcriptional and post-transcriptional responses. Our results do not distinguish between the different mechanisms described above; instead, they indicate that these are mechanisms that should be investigated. The emergence of zebrafish oligonucleotide microarrays, proteomics, and the development of MO and transgenic techniques should allow rapid progress toward understanding the molecular mechanisms that lead to TCDD embryotoxicity in zebrafish.

Acknowledgments

We thank the entire Peterson/Heideman fish lab, especially Amy Prasch, for their insight and advice throughout this project. We also thank Dr. John Stegeman (Woods Hole Oceanographic Institution) for the generous supply of mAb 1-12-3 antibody. We acknowledge P. Black, E. S. Fluegel, J. L. Hooker, and D. Nesbit for expert assistance and support. Contribution 357, Molecular and Environmental Toxicology Center, University of Wisconsin, Madison, WI 53706.

References

- Andreasen EA, Hahn ME, Heideman W, Peterson RE, and Tanguay RL (2002a) The zebrafish (*Danio rerio*) aryl hydrocarbon receptor type 1 is a novel vertebrate receptor. *Mol Pharmacol* **62**:234–249.
- Andreasen EA, Spitsbergen JM, Tanguay RL, Stegeman JJ, Heideman W, and Peterson RE (2002b) Tissue-specific expression of AHR2, ARNT2 and CYP1A in zebrafish embryos and larvae: effects of developmental stage and 2,3,7,8-tetrachlorodibenzo-*p*-dioxin exposure. *Toxicol Sci* **68**:403–419.
- Belair CD, Peterson RE, and Heideman W (2001) Disruption of erythropoiesis by dioxin in the zebrafish. *Dev Dyn* **222**:581–594.
- Borlakoglu JT, Stegeman J, and Dils RR (1991) Induction of hepatic cytochrome P-450A1 in pigeons treated *in vivo* with Aroclor 1254, a commercial mixture of polychlorinated biphenyls (PCBs). *Comp Biochem Physiol C* **99**:279–286.
- Cantrell SM, Joy-Schleizinger J, Stegeman JJ, Tillitt DE, and Hannink M (1998) Correlation of 2,3,7,8-tetrachlorodibenzo-*p*-dioxin-induced apoptotic cell death in the embryonic vasculature with embryotoxicity. *Toxicol Appl Pharmacol* **148**:24–34.
- Cantrell SM, Lutz LH, Tillitt DE, and Hannink M (1996) Embryotoxicity of 2,3,7,8-tetrachlorodibenzo-*p*-dioxin (TCDD): the embryonic vasculature is a physiological target for TCDD-induced DNA damage and apoptotic cell death in medaka (*Oryzias latipes*). *Toxicol Appl Pharmacol* **141**:23–34.
- Carlson DB and Perdew GH (2002) A dynamic role for the AH receptor in cell signaling? Insights from a diverse group of AH receptor interacting proteins. *J Biochem Mol Toxicol* **16**:317–325.
- Cook PM, Robbins JA, Endicott DD, Lodge KB, Guiney PD, Walker MK, Zabel EW, and Peterson RE (2003) Effects of aryl hydrocarbon receptor-mediated early life stage toxicity on lake trout populations in Lake Ontario during the 20th century. *Environ Sci Technol* **37**:3864–3877.
- Dalton TP, Puga A, and Shertzer HG (2002) Induction of cellular oxidative stress by aryl hydrocarbon receptor activation. *Chem Biol Interact* **141**:77–95.
- Dong W, Teraoka H, Tsujimoto Y, Stegeman JJ, and Hiraga T (2004) Role of aryl hydrocarbon receptor in mesencephalic circulation failure and apoptosis in zebrafish embryos exposed to 2,3,7,8-tetrachlorodibenzo-*p*-dioxin. *Toxicol Sci* **77**:109–116.
- Dong W, Teraoka H, Yamazaki K, Tsukiyama S, Imani S, Imagawa T, Stegeman JJ, Peterson RE, and Hiraga T (2002) 2,3,7,8-Tetrachlorodibenzo-*p*-dioxin toxicity in the zebrafish embryo: local circulation failure in the dorsal midbrain is associated with increased apoptosis. *Toxicol Sci* **69**:191–201.
- Drahushuk AT, McGarrigle BP, Larsen KE, Stegeman JJ, and Olson JR (1998) Detection of CYP1A1 protein in human liver and induction by TCDD in precision-cut liver slices incubated in dynamic organ culture. *Carcinogenesis* **19**:1361–1368.
- Fisher JM, Wu L, Denison MS, and Whitlock JP (1990) Organization and function of a dioxin-responsive enhancer. *J Biol Chem* **265**:9676–9681.
- Frueh FW, Hayashibara KC, Brown PO, and Whitlock JP (2001) Use of cDNA microarrays to analyze dioxin-induced changes in human liver gene expression. *Toxicol Lett* **122**:189–203.
- Guiney PD, Smolowitz RM, Peterson RE, and Stegeman JJ (1997) Correlation of 2,3,7,8-tetrachlorodibenzo-*p*-dioxin induction of cytochrome P4501A in vascular endothelium with toxicity in early life stages of lake trout. *Toxicol Appl Pharmacol* **143**:256–273.
- Guiney PD, Walker MK, Spitsbergen JM, and Peterson RE (2000) Hemodynamic dysfunction and cytochrome P4501A mRNA expression induced by 2,3,7,8-tetrachlorodibenzo-*p*-dioxin during embryonic stages of lake trout development. *Toxicol Appl Pharmacol* **168**:1–14.
- Hahn ME (1998) The aryl hydrocarbon receptor: a comparative perspective. *Comp Biochem Physiol C* **121**:23–53.
- Hakansson H, Johansson L, Manzoor E, and Ahlberg UG (1994) Effect of 2,3,7,8-tetrachlorodibenzo-*p*-dioxin on the hepatic 7-ethoxyresorufin *O*-deethylase activity in four rodent species. *Eur J Pharmacol* **270**:279–284.
- Henry TR, Spitsbergen JM, Hornung MW, Abnet CC, and Peterson RE (1997) Early life stage toxicity of 2,3,7,8-tetrachlorodibenzo-*p*-dioxin in zebrafish (*Danio rerio*). *Toxicol Appl Pharmacol* **142**:56–68.
- Huang YW, Stegeman JJ, Woodin BR, and Karasov WH (2001) Immunohistochemical localization of cytochrome P4501A induced by 3,3',4,4',5-pentachlorobiphenyl (PCB 126) in multiple organs of northern leopard frogs, *Rana pipiens*. *Environ Toxicol Chem* **20**:191–197.
- Hytti OM, Nyman M, Willis ML, Raunio H, and Pelkonen O (2001) Distribution of cytochrome P4501A (CYP1A) in the tissues of Baltic ringed and grey seals. *Marine Environmental Research* **51**:465–485.
- Morrison HG, Weil EJ, Karchner SI, Sogin ML, and Stegeman JJ (1998) Molecular cloning of CYP1A from the estuarine fish *Fundulus heteroclitus* and phylogenetic analysis of CYP1 genes: update with new sequences. *Comp Biochem Physiol C* **121**:231–240.
- Nacci D, Coiro L, Kuhn A, Champlin D, Munns W, Specker J, and Cooper K (1998) Nondestructive indicator of ethoxyresorufin-*O*-deethylase activity in embryonic fish. *Environ Toxicol Chem* **17**:2481–2486.
- Nasevicius A and Ekker SC (2000) Effective targeted gene 'knockdown' in zebrafish. *Nat Genet* **26**:216–220.
- Nebert DW, Petersen DD, and Fornace AJ (1990) Cellular responses to oxidative stress: the [Ah] gene battery as a paradigm. *Environ Health Perspect* **88**:13–25.
- Park SS, Miller H, Klotz AV, Kloepper-Sams PJ, Stegeman JJ, and Gelboin HV (1986) Monoclonal antibodies to liver microsomal cytochrome P-450E of the marine fish *Stenotomus chrysops* (scup): cross reactivity with 3-methylcholanthrene induced rat cytochrome P-450. *Arch Biochem Biophys* **249**:339–350.
- Prasch AL, Teraoka H, Carney SC, Dong W, Hiraga T, Stegeman JJ, Heideman W, and Peterson RE (2003) Aryl hydrocarbon receptor 2 mediates 2,3,7,8-tetrachlorodibenzo-*p*-dioxin developmental toxicity in zebrafish. *Toxicol Sci* **76**:138–150.
- Puga A, Maier A, and Medvedovic M (2000) The transcriptional signature of dioxin in human hepatoma HepG2 cells. *Biochem Pharmacol* **60**:1129–1142.
- Rowlands JC and Gustafsson JA (1997) Aryl hydrocarbon receptor-mediated signal transduction. *Crit Rev Toxicol* **27**:109–134.
- Schleizinger JJ, Keller J, Verbrugge LA, and Stegeman JJ (2000) 3,3',4,4'-tetrachlorobiphenyl oxidation in fish, bird and reptile species: relationship to cytochrome P450 1A inactivation and reactive oxygen production. *Comp Biochem Physiol C* **125**:273–286.
- Schmidt JV and Bradfield CA (1996) Ah receptor signaling pathways. *Annu Rev Cell Dev Biol* **12**:55–89.
- Simanainen U, Tuomisto JT, Tuomisto J, and Viluksela M (2003) Dose-response analysis of short-term effects of 2,3,7,8-tetrachlorodibenzo-*p*-dioxin in three differentially susceptible rat lines. *Toxicol Appl Pharmacol* **187**:128–136.
- Smith AG, Clothier B, Carthew P, Childs NL, Sinclair PR, Nebert DW, and Dalton TP (2001) Protection of the *cyp1a2*(–/–) null mouse against uroporphyrin and hepatic injury following exposure to 2,3,7,8-tetrachlorodibenzo-*p*-dioxin. *Toxicol Appl Pharmacol* **173**:89–98.
- Tanguay RL, Andreasen EA, Walker MK, and Peterson RE (2003) Dioxin toxicity and aryl hydrocarbon receptor signaling in fish, in *Dioxins and Health* (Schechter A and Gasiewicz TA eds) pp 603–628, John Wiley & Sons, Inc., New Jersey.
- Teraoka H, Dong W, Ogawa S, Tsukiyama S, Okuhara Y, Niiyama M, Ueno N, Peterson RE, and Hiraga T (2002) 2,3,7,8-Tetrachlorodibenzo-*p*-dioxin toxicity in the zebrafish embryo: altered regional blood flow and impaired lower jaw development. *Toxicol Sci* **65**:192–199.
- Teraoka H, Dong W, Tsujimoto Y, Iwasa H, Endoh D, Ueno N, Stegeman JJ, Peterson RE, and Hiraga T (2003) Induction of cytochrome P450 1A is required for circulation failure and edema by 2,3,7,8-tetrachlorodibenzo-*p*-dioxin in zebrafish. *Biochem Biophys Res Commun* **304**:223–228.
- Toomey BH, Bello S, Hahn ME, Cantrell S, Wright P, Tillitt DE, and Di Giulio RT (2001) 2,3,7,8-Tetrachlorodibenzo-*p*-dioxin induces apoptotic cell death and cytochrome P4501A expression in developing *Fundulus heteroclitus* embryos. *Aquat Toxicol* **53**:127–138.
- Tuomisto JT, Viluksela M, Pohjanvirta R, and Tuomisto J (1999) The AH receptor and a novel gene determine acute toxic responses to TCDD: segregation of the resistant alleles to different rat lines. *Toxicol Appl Pharmacol* **155**:71–81.
- Uno S, Dalton TP, Senft AP, Shertzer HG, and Nebert DW (2002) *Cyp1a1* (–/–) knockout mice, which have a functional aromatic hydrocarbon receptor, are protected against dioxin, as well as benzo(a)pyrene, toxicity in specific tissues. *Toxicol Sci Suppl* **66**:21.
- Walker MK and Peterson RE (1994) Aquatic toxicity of dioxins and related chemicals, in *Dioxins and Health* (Schechter A ed) pp 347–387, Plenum Press, New York.
- Westerfield M (1995) *The Zebrafish Book*. University of Oregon Press, Eugene.
- Wisk JD and Cooper KR (1990) The stage specific toxicity of 2,3,7,8-tetrachlorodibenzo-*p*-dioxin in embryos of the Japanese medaka (*Oryzias latipes*). *Environ Toxicol Chem* **9**:1159–1169.

Address correspondence to: Warren Heideman, School of Pharmacy, University of Wisconsin, 777 Highland Avenue, Madison, WI 53705. E-mail: wheidema@wisc.edu